

Mean-Field HP Model, Designability and Alpha-Helices in Protein Structures

C. T. Shih,¹ Z. Y. Su,¹ J. F. Gwan,¹ B. L. Hao,^{2,3} C. H. Hsieh,¹ and H. C. Lee^{3,4}

¹National Center for High-Performance Computing, Hsinchu, Taiwan, Republic of China

²Institute of Theoretical Physics, Academia Sinica, Beijing, China

³National Center for Theoretical Sciences, Hsinchu, Taiwan, Republic of China

⁴Department of Physics and Center for Complex Systems, National Central University, Chungli, Taiwan, Republic of China

(Received 9 November 1998)

Analysis of the geometric properties of a mean-field HP model on a square lattice for protein structure shows that structures with a large number of switchbacks between surface and core sites are chosen favorably by peptides as unique ground states. Global comparison of model (binary) peptide sequences with concatenated (binary) protein sequences listed in the Protein Data Bank and the Dali Domain Dictionary indicates that the highest correlation occurs between model peptides choosing the favored structures and those portions of protein sequences containing alpha helices.

PACS numbers: 87.10.+e, 87.15.By

The three-dimensional structure of proteins is a complex physical and mathematical problem of prime importance in molecular biology, medicine, and pharmacology [1]. It is believed that the folding instruction of a protein is encoded in its amino acid sequence [2] and from model studies much has been learned about protein structure and folding kinetics [3–6]. Yet much still remains to be understood. This simple fact is already intriguing: the number of possible globular structures for a peptide of typical length—about 300 amino acids—is practically infinite; the number of proteins whose structures are known empirically or hypothetically is more than 100 000 and is growing rapidly with time; the number of classes of native protein structures is about 500 and is believed unlikely to exceed 1000 in the long run [1,7]. Numerical simulations based on lattice models have shown that structures of exceptionally high *designability*—those that attract a large number of protein sequences to conform to it—do exist [5,6,8]. Why such structures would emerge is, however, not well understood. Protein folding also has an outstanding temporal feature: the initial collapse to globular shape and the formation of α helices are completed in less than 10^{-7} sec [9], while the rest of the folding takes up to 10 sec to complete.

In this Letter, based on results from a mean-field lattice model we observe that high-designability structures are preponderant in a type of substructure that suggests α helices in real proteins and we explain the reason behind this phenomenon. This notion is supported by global comparisons of model peptides that fold into high-designability structures with (binary) sequences constructed from nonredundant sets of proteins in the Protein Data Bank (PDB) [10] and the Dali Domain Dictionary (DDD) [7]. Since the mean field in the model represents the hydrophobic potential that is known to cause the initial collapse of a peptide to a globular shape, the results may explain why the initial collapse *and* the formation of α helices occur essentially simultaneously and rapidly, and are temporally

separated from other slower folding processes that are driven by far-neighbor inter-residual interactions.

In the *HP* model of Dill *et al.* [3], the 20 kinds of amino acids are divided into two types, hydrophobic and polar. This reduces a peptide chain of length N to a binary “peptide” $\mathbf{p} = (p_1, p_2, \dots, p_N)$, where $p_i = 0$ (1) if the amino acid at the i th position on the chain is polar (hydrophobic). A structure is represented by a self-avoiding path compactly embedded on a lattice \mathcal{L} , and the energy associated with a peptide conforming to a particular structure is computed from the contact energies between the nearest-neighbor residues that are not adjacent along the peptide. A set of well tested contact energies derived from proteins of known structure is the Miyazawa-Jernigan matrix, which is, however, well approximated by an effective mean-field potential expressing the hydrophobicities of the residues [11]. In the binary form of this approximation the Hamiltonian of the HP model is reduced to that of a mean-field model [5,12],

$$H(\mathbf{p}, \mathbf{s}) = -\mathbf{p} \cdot \mathbf{s} = \frac{1}{2} (|\mathbf{s} - \mathbf{p}|^2 - \mathbf{p}^2 - \mathbf{s}^2), \quad (1)$$

where $\mathbf{s} = (s_1, s_2, \dots, s_N)$ is a binary “structure” converted from a self-avoiding path with the assignment: $s_i = 1$ (0) if the i th site is a core (surface) site on the lattice. Empirical observation suggests that protein folding proceeds in two steps, a first stage of fast collapse and formation of alpha helices (and probably some not properly folded beta sheets) presumably caused mainly by hydrophobic interactions under polymeric constraints, followed by a second stage of slow annealing caused by far-neighbor inter-residue interactions leading to the final native state [9,13]. Since Eq. (1) is a local, mean-field approximation that leaves out residual—i.e., left over from mean-field averaging—far-neighbor interactions, it can be relied on to account for only the first stage.

We denote by S the set of all distinct structures \mathbf{s} on \mathcal{L} and by \mathcal{P} the set of all possible peptides \mathbf{p} of length

N . For each \mathbf{p} the selection of the \mathbf{s} giving the minimum H defines a mapping from \mathcal{P} to \mathcal{S} . There are \mathbf{p} 's that are mapped to more than one \mathbf{s} or are mapped to \mathbf{s} 's that correspond to more than one self-avoiding path. Such \mathbf{p} 's are removed from \mathcal{P} and their target \mathbf{s} 's are removed from the competition for high designability, because a peptide that does not conform to a unique structure at all times is not expected to survive the evolutionary selection process [14,15]. It has also been shown that not admitting degenerate states in a coarse-grained model is similar to removing peptides that have low foldability in a finer-grained model [16]. (Many states that are degenerate in the present coarse-grained model would in a model with higher energy resolution be states of different symmetries with nearly degenerate energies. The energy landscape for the ground state among these would likely contain deep local minima, and a peptide choosing such a ground state would likely be a poor folder.) The mapping then partitions what remains in \mathcal{P} into classes, with all the \mathbf{p} 's in each class mapped to a single \mathbf{s} , whose designability is simply the number of \mathbf{p} 's in the class. For this mapping the right-hand side of Eq. (1) reduces to being proportional to $|\mathbf{s} - \mathbf{p}|^2$, the Hamming distance between the two points \mathbf{p} and \mathbf{s} in an N -dimensional unit hypercube. Then the designability of an \mathbf{s} is essentially the Voronoi polytope around it in this hypercube [12].

Excepting those peptides removed for degeneracy, \mathcal{P} is just the set of all the vertices on a unit hypercube. In comparison, owing to the constraints of compactness and self-avoidance imposed on paths on \mathcal{L} , points in \mathcal{S} are sparsely distributed in the hypercube so that $\mathcal{S} \subset \mathcal{P}$. For example, on a 6×6 square lattice, the number of elements in (including those to be removed for degeneracies) \mathcal{P} is $2^{36} = 68\,719\,476\,736$, while those in \mathcal{S} are 30 408 (but only 18 213 of them have no path degeneracy). If the points in \mathcal{S} were uniformly distributed in the hypercube, then the Voronoi polytope around each \mathbf{s} would be the same and every \mathbf{s} would have the same designability. But owing to boundary effects and geometric constraints imposed on the compact paths on \mathcal{L} , the distribution of \mathbf{s} 's in \mathcal{S} cannot be uniform, those \mathbf{s} 's residing in regions in the hypercube that are of especially low density (in \mathbf{s} 's) will then have especially high designability.

We now examine how geometric constraints cause the emergence of \mathbf{s} 's with especially high designabilities by first attempting to replace the constraints with a set of explicit algebraic "rules." Consider a structure in \mathcal{S} to be a chain of 0's and 1's linked by $N - 1$ links of three types, 0-0, 1-0 or 0-1, 1-1, with n_{00} , n_{10} , and n_{11} being the numbers of such links, respectively. The structure is partitioned by the 1-0 links into $n_{10} + 1$ "islands" of contiguous 1's or 0's. (Peptides in \mathcal{P} may be similarly described, but the only constraint on any \mathbf{p} is that the total number of 0's and 1's be N .) For \mathcal{L} being a square lattice with side L , two of the most important constraining rules are (i) a single 0 may occur only at an end of a

path, and (ii) an isolated single 1 may only either occur at or be one 0-island away from an end of a path. Space does not allow us to give more than one other relatively simple example (with $L > 4$): For a path having the pattern $\mathbf{s} = (1 \dots 1)$ (both the ends of the path are 1-sites), $2n_{00} + n_{10} = 8L - 8$ and $2 \leq n_{10} \leq 4L - 12$. It is, in fact, extremely difficult if not impossible to exhaust the complete set of such rules needed to reduce \mathcal{P} to \mathcal{S} [17]. For our purpose it suffices to identify a large enough set of rules which reduces \mathcal{P} to a \mathcal{S}' that is sufficiently close to \mathcal{S} for us to understand the origin and characteristics of structures of high designability.

In Fig. 1(a) the number of peptides in \mathcal{P} (open circle) and structures in \mathcal{S}' (solid circle) and \mathcal{S} (open triangle) on a 6×6 lattice are plotted against n_{10} . The total number of elements under the curve for \mathcal{P} gives the total number of sites in the hypercube. \mathcal{S}' is slightly greater than \mathcal{S} but is much smaller than \mathcal{P} . (The boundary of \mathcal{S}' owes its roughness to the incompleteness of the set of rules used to construct it.) It is seen that, whereas for \mathcal{P} the maximum possible value for n_{10} is $4L - 4 = 32$, for \mathcal{S} and \mathcal{S}' the corresponding maximum is much less: $n_{\max} = 14$. As n_{10} approaches n_{\max} from below, the number of elements in

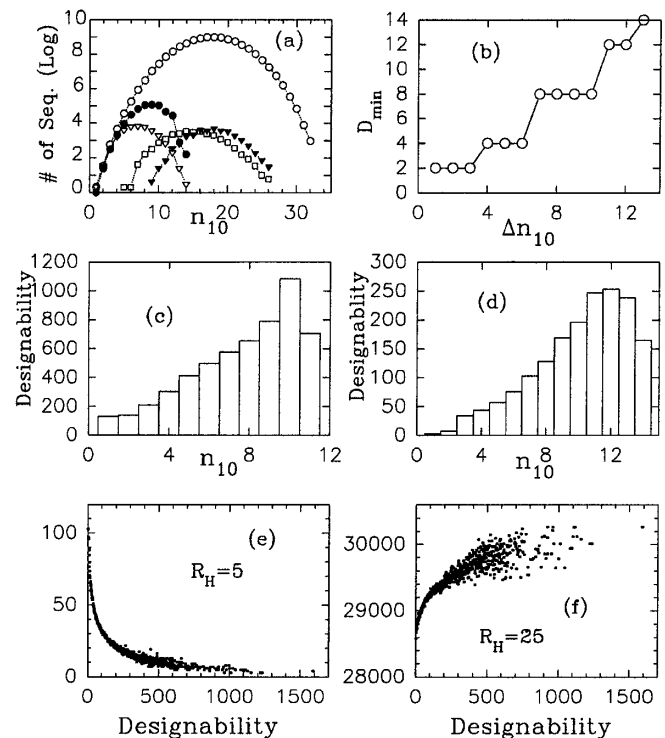


FIG. 1. (a) Number of peptides vs n_{10} for \mathcal{P} (open circle), \mathcal{P}_4 (solid triangle), and \mathcal{P}_5 (square), and number of structures vs n_{10} for \mathcal{S}' (solid circle) and \mathcal{S} (open triangle), on the 6×6 lattice. (b) Smallest Hamming distance vs differences of n_{10} of all the 30 408 paths in \mathcal{P} on the 6×6 lattice. Average designabilities of the paths vs n_{10} for the (c) 4×7 and (d) 6×6 lattices, respectively. Number of neighboring structures within a Hamming distance of (e) $R_H = 5$ and (f) $R_H = 25$ of a structure of given designability.

S' decreases rapidly, whereas those in \mathcal{P} increase toward a maximum. It happens that in the hypercube the smallest Hamming distance between two structures is approximately proportional to the difference in their respective n_{10} numbers. This is evident in Fig. 1(b), where the smallest Hamming distance is plotted against the difference in n_{10} for all the pairs among the 30408 binary structures on a 6×6 lattice, and is consistent with results given in [18] in which $x(p)$ (the degree of clustering of hydrophobic residues) is analogous to n_{10} .

Since allowed structures with n_{10} 's having values close to n_{\max} live in a region of the hypercube that is not only especially sparse in \mathbf{s} 's but also most dense in \mathbf{p} 's, it follows that they would on average have a large Voronoi polytope, and hence are most likely to have the highest designabilities. This is substantially borne out by the results shown in Figs. 1(c) and 1(d) computed for the allowed structures on the 4×7 and 6×6 lattices, respectively, where average designability is plotted against n_{10} . The average designability does not exactly peak at $n_{10} = n_{\max}$ but rather at n_{10} 's just less than n_{\max} . Why this should be so is not yet clearly understood. Structures with maximum n_{10} are the most constrained and are very few in number so that otherwise secondary details might have had a larger effect on their designabilities. Preference for large n_{10} 's has also been observed on other 2D and 3D lattices. The relation between high designability and sparse population is further illustrated in Figs. 1(e) and 1(f), where the number of structures within a Hamming distance R_H of a given structure is plotted against the designability of that structure. In 1(e), where $R_H = 5$, it is seen that structures with high designability have far fewer near neighbors than structures with low designability. In 1(f), where $R_H = 25$, it is seen that all structures have approximately the same large numbers of near and far neighbors.

Now something interesting emerges. A structure with its n_{10} (almost) maximized but not allowed to have single 1's or 0's except at its ends [rules (i) and (ii)] will have a preponderance of the 4-mer (1100) in the interior, so that large stretches of it will have the form (...11001100...) which suggests the linear structure of α helices on a lattice. A corollary is that structures with core to surface ratios close to unity are favored by designability. This implies a diameter of approximately 10 residues for an ideal protein, which is consistent with the typical size of 300 to 1000 amino acids in natural proteins. Note that the selection of structures with maximized n_{10} is a consequence of the geometric property of the Hamiltonian (1) in hyperspace and does not depend on the specifics of a lattice. That larger n_{10} 's are favored is a notion qualitatively consistent with the conclusion drawn from recent studies on folding kinetics that optimal structures are also minimally frustrated [15].

To see if what we have observed so far has anything to do with real proteins we compare five sequences, \mathcal{P}_{1-5} , each being a concatenation of a set of real protein or

(6×6) lattice binary peptides: \mathcal{P}_1 , (a) the representative nonredundant 2886 proteins (sequence similarity smaller than 90%) [19] culled from the 9257 entries in PDB [10], or (b) the even less redundant set of 1394 entries of protein domains from DDD [7], converted to binary sequences based on hydrophobicity [20]; \mathcal{P}_2 , the sections in \mathcal{P}_1 that fold into α helices; \mathcal{P}_3 , the sections in \mathcal{P}_1 that fold into β sheets; \mathcal{P}_4 , the 27006 peptides in \mathcal{P} mapped to the 15 structures of the highest designabilities; \mathcal{P}_5 , the 24134 peptides in \mathcal{P} mapped to the 1545 structures of the lowest designabilities. Interestingly, the H/P ratios of the five sequences are all very close to 1; the percentage of hydrophobic residues contained in each is, respectively, 50.00%, 49.75%, 56.18%, 50.43%, and 49.05% for \mathcal{P}_1 (from PDB; numbers from DDD are similar) through \mathcal{P}_5 . Figure 1(a) shows that neither distribution of peptides in \mathcal{P}_4 (solid triangle) and \mathcal{P}_5 (open square) vs n_{10} is random, which corroborates the results of [21]. In particular, in \mathcal{P}_5 (\mathcal{P}_4) peptides with larger (smaller) n_{10} 's are slightly favored over those with smaller (larger) n_{10} 's.

Let $f_i^{(l)}(m)$ be the frequency, normalized to that of a sequence with an H/P ratio of unity (if the word has n_H H 's and the actual frequency of the word is f , then the normalized frequency is $(n_H/n_P)^{-n_H} f$), of the m th binary word of length l occurring in sequence \mathcal{P}_i and let $F_i^{(l)}(m) = [f_i^{(l)}(m) - \bar{f}_i^{(l)}]/Z$ be the normalized frequency distribution function, where $\bar{f}_i^{(l)} = 2^{-l} \sum_m f_i^{(l)}(m)$ is the mean frequency and $Z = \{\sum_m [f_i^{(l)}(m) - \bar{f}_i^{(l)}]^2\}^{1/2}$ is the norm. The relations $\sum_m F_i^{(l)}(m) = 0$ and $\sum_m [F_i^{(l)}(m)]^2 = 1$ hold. The pairwise overlaps $O_{ij}^{(l)} = \sum_{m=1}^{2^l} F_i^{(l)}(m) F_j^{(l)}(m)$; $i = 1, 2, 3$; $j = 4, 5$ that measure correlations between \mathcal{P}_i and \mathcal{P}_j for $l = 4-14$ are given in Figs. 2(a) and 2(b), where the real protein sequences used are from PDB and DDD, respectively. The two sets of overlaps are qualitatively similar. It is seen that

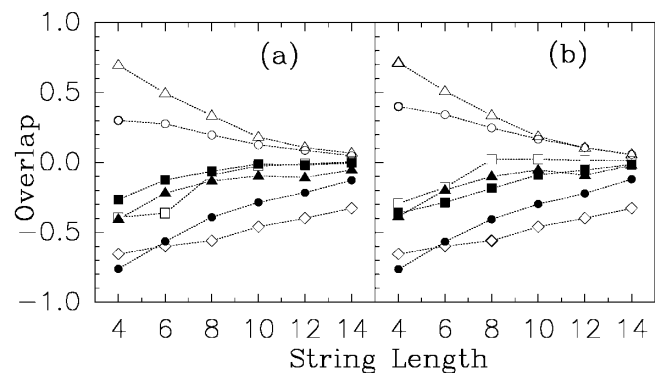


FIG. 2. Overlap of frequency distribution functions of lattice peptides and PDB proteins (a) and DDD protein domains (b) as a function of word length l : $O_{14}^{(l)}$ (open circle), $O_{15}^{(l)}$ (solid circle), $O_{24}^{(l)}$ (open triangle), $O_{25}^{(l)}$ (solid triangle), $O_{34}^{(l)}$ (open square), $O_{35}^{(l)}$ (solid square), and $O_{45}^{(l)}$ (open diamond).

\mathcal{P}_4 (\mathcal{P}_5) is positively (negatively) correlated with \mathcal{P}_1 and \mathcal{P}_2 . For all values of l the strongest correlation occurs between the model sequence of high designability (\mathcal{P}_4) and the real protein sequence rich in α helices (\mathcal{P}_2). The sequence of high designability is poorly correlated with the sequence rich in β sheets (\mathcal{P}_3) and, as expected, the strongest anticorrelation occurs between the two model sequences of high (\mathcal{P}_4) and low (\mathcal{P}_5) designabilities.

Even though the favoring of surface-core repeats by peptides folding into high-designability structures is most likely not lattice specific (provided the H/P ratio is close to one), the particular choice of the (1100) repeat has the characteristic of a square lattice. For instance, on a hexagonal lattice the predominant repeat would more likely be (10) rather than (1100). There is some justification for selecting square lattices over hexagonal because in real proteins the backbone does not favor small-angle bends. On the other hand, real proteins do not live on lattices and the equivalent of (10) repeats does occur in real proteins where β sheets are exposed to solvent. Thus the low correlation between \mathcal{P}_3 and \mathcal{P}_4 is to some extent an artifact of the square lattice, and it may be better to interpret the (1100) repeats on a square lattice as representing α type and some β type repeats (but not the latter's foldings) in real proteins.

Our study suggests that the rough formation of α helices and some β sheets and the collapse of proteins into globular shapes are primarily determined by hydrophobicity. Since only the mean-field part of the inter-residue interaction is included in the model, this implies that details of the residual inter-residue interaction that determine the final shape of the native state are not important at this stage. It has been pointed out that structures of high designability in a lattice model with two-letter amino acid alphabet may not be especially designable for higher-letter alphabets [16]. Although the situation may be different on a lattice larger than the 5×5 lattice used in [16], it does remain to be verified whether our findings persist in finer-grained and more realistic models. If it does, then we can better understand why the formation of α helices and the collapse would happen on a similar time scale, of the order 10^{-7} sec, why the formation of β sheets would take somewhat longer (about 10^{-6} sec) [9,13], and why these time scales would be so much shorter than the time needed to complete the rest of the folding (10^{-1} to 10 sec). This scenario is in any case consistent with the finding in a recent statistical analysis of experimental data: local contacts play the key role in fast processes during folding [22].

This work is partly supported by Grants No. NCHC88-CP-A001 to ZYS from the National Center for High-Performance Computing, and No. NSC87-M-2112-008-002 to H.C.L. and No. NSC87-M-2112-007-004 to B.L.H. from the National Science Council (ROC). H.C.L. thanks Simon Fraser University for

hospitality in the summer of 1998 during which part of the paper was written.

-
- [1] *Protein Folding*, edited by T.E. Creighton (W.H. Freeman and Company, New York, 1992); C. Chothia, *Nature* (London) **357**, 543–544 (1992).
 - [2] C. Anfinsen, *Science* **181**, 223 (1973).
 - [3] K.A. Dill, *Biochemistry* **24**, 1501 (1985); H.S. Chan and K.A. Dill, *Macromolecules* **22**, 4559 (1989).
 - [4] E.I. Shakhnovich, *Phys. Rev. Lett.* **72**, 3907 (1994); P.G. Wolynes, J.N. Onuchic, and D. Thirumalai, *Science* **267**, 1619 (1995); H.S. Chan and K.A. Dill, *Proteins* **24**, 335 (1996).
 - [5] H. Li, R. Helling, C. Tang, and N.S. Wingreen, *Science* **273**, 666 (1996).
 - [6] E.I. Shakhnovich, *Curr. Biol.* **8**, R478 (1998).
 - [7] L. Holm and C. Sander, *Nucl. Acids Res.* **26**, 316 (1998); *Proteins* **33**, 88 (1998); the website www2.ebi.ac.uk/dali/domain/2.0/DDD.fasta.
 - [8] D.J. Lipman and W.J. Wilbur, *Proc. R. Soc. London* **245**, 7 (1991); S. Govindarajan and R.A. Goldstein, *Biopolymers* **36**, 43 (1995); *Proc. Natl. Acad. Sci. U.S.A.* **93**, 3341 (1996); M.R. Ejtehadi, N. Hamedani, H. Seyed-Allaei, V. Shahrezaei, and M. Yahyanejad, *Phys. Rev. E* **57**, 3298 (1998).
 - [9] V. Muñoz, P.A. Thomson, J. Hofrichter, and W.A. Eaton, *Nature* (London) **390**, 196 (1997).
 - [10] Protein Data Bank, ver.87, released Jan. 1999.
 - [11] S. Miyazawa and R.L. Jernigan, *J. Mol. Biol.* **256**, 623 (1996); H. Li, C. Tang, and N.S. Wingreen, *Phys. Rev. Lett.* **79**, 765 (1997); O. Keskin *et al.*, *Protein Sci.* **7**, 2578 (1998); Z.H. Wang and H.C. Lee, LANL e-print xxx.lanl.gov/cond-mat/9907432.
 - [12] H. Li, R. Helling, C. Tang, and N.S. Wingreen, *Proc. Natl. Acad. Sci. U.S.A.* **95**, 4987 (1998).
 - [13] S. Williams *et al.*, *Biochemistry* **35**, 691 (1996).
 - [14] S.S. Plotkin, J. Wang, and P.G. Wolynes, *J. Chem. Phys.* **106**, 2932 (1997); M. Cieplak and T.X. Hoang, *Phys. Rev. E* **58**, 3589 (1998).
 - [15] J.D. Bryngleson and P.G. Wolynes, *Biopolymers* **30**, 177 (1990); E.D. Nelson, L.F. Teneyck, and J.N. Onuchic, *Phys. Rev. Lett.* **79**, 3534 (1997); H. Nymeyer, A.E. Garcia, and J.N. Onuchic, *Proc. Natl. Acad. Sci. U.S.A.* **95**, 5921 (1998).
 - [16] N.E.G. Buchler and R.A. Goldstein, *Proteins* **34**, 113 (1999).
 - [17] M.R. Garey and D.S. Johnson, *Computers and Intractability, A Guide to the Theory of NP-Completeness* (W.H. Freeman, New York, 1979).
 - [18] E.D. Nelson and J.N. Onuchic, *Proc. Natl. Acad. Sci. U.S.A.* **95**, 10682 (1998).
 - [19] L. Holm and C. Sander, *Bioinformatics* **14**, 423 (1998).
 - [20] A. Radzicka *et al.*, *Biochemistry* **27**, 1664 (1988).
 - [21] A. Irbäck and F. Potthast, *J. Chem. Phys.* **103**, 10298 (1995); A. Irbäck, C. Peterson, and F. Potthast, *Proc. Natl. Acad. Sci. U.S.A.* **93**, 9533 (1996); E.D. Nelson, L.F. Ten Eyck, and N. Onuchic, LANL e-print physics/9812048.
 - [22] K.W. Plaxco, K.T. Simons and D. Baker, *J. Mol. Biol.* **277**, 985 (1998); H.S. Chan, *Nature* (London) **392**, 761 (1998).